2013-01-01

Quark Fluctuations in a Chiral Model in the Presence of a Magnetic Field

Lidens Cheng
University of Texas at El Paso, lcheng2@miners.utep.edu

QUARK FLUCTUATIONS IN A CHIRAL MODEL IN THE PRESENCE OF A MAGNETIC FIELD

LIDENS CHENG

Department of Physics

APPROVED:

Vivian Incera, Ph.D., Chair

Efrain Ferrer, Ph.D.

Vladik Kreinovich, Ph.D

Benjamin C. Flores, Ph.D.
Dean of the Graduate School

QUARK FLUCTUATIONS IN A CHIRAL MODEL IN THE PRESENCE OF A MAGNETIC FIELD

By

LIDENS CHENG

THESIS

Presented to the Faculty of the Graduate School of

The University of Texas at El Paso

in Partial Fulfillment

of the Requirements

for the Degree of

MASTER OF SCIENCE

Department of Physics

THE UNIVERSITY OF TEXAS AT EL PASO

May 2013

Table of Contents

List of Figures

1 Introduction

The quantum chromodynamics (QCD) phase diagram is the scheme that delineates the boundaries of different phases that can exist at finite temperature and baryonic chemical potential for strongly interacting matter. In the temperature-chemical potential plane, the two extremes of the QCD phase diagram are well understood [1, 2]. The quark-gluon plasma (QGP) phase is located at the high-temperature/low-chemical potential corner while the color-flavor-locking (CFL) phase is located at low-temperature/high-chemical potential corner. In those extremes, due to the large energy scales, the coupling constant runs to small values due to asymptotic freedom. Hence, it is natural to expect that in the regions of intermediate temperature and chemical potential, a phase transition occurs from a confined phase to a deconfined phase where quarks and gluons are liberated from hadrons.

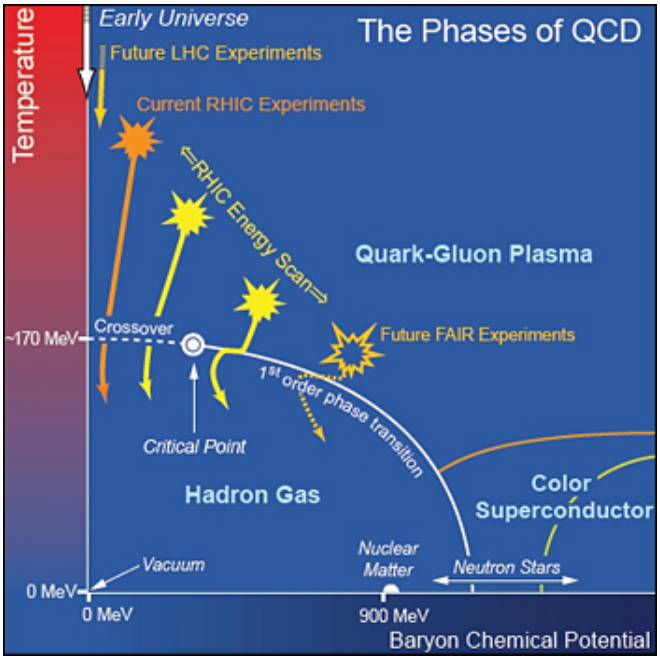

Figure 1.1: QCD phase diagram in the temperature-chemical potential plane

Although confined quarks have a large dynamical mass, the quark mass becomes small in the regions of small coupling. Thus, by increasing temperature or chemical potential, a phase transition should occur from the phase of heavy quarks to that of light quarks. From lattice calculations [3], it is known that for physical values of the quark masses at vanishing chemical potential and increasing temperature, the change from hadronic matter to QGP is a rapid crossover. On the other hand, at zero temperature and increasing chemical potential, the transition between the same two phases has been found to be first order [4, 5, 6, 7]. It is then expected that somewhere in the interior of the phase diagram a critical point (CP) must exist where the first-order transition turns into a crossover or into a second-order transition if the light quark masses are neglected [8, 9, 10, 11].

Understanding the nature of the chiral and deconfinement phase transitions, the location of the CP, and the properties in its vicinity are among the most important problems in the field of QCD. The purpose of this thesis is to use the two-flavor Nambu-Jona-Lasinio (NJL) model in the presence of a magnetic field at the chiral limit to study the phase boundary where the spontaneously broken chiral symmetry is restored. At small chemical potential, the phase boundary exhibits a second-order phase transition. On the other hand, at large chemical potential and appropriate coupling constant, the phase boundary exhibits a first-order phase transition [12]. Therefore, a tricritical point (TCP) is expected along the phase boundary where the order of the phase transition changes. The addition of a strong magnetic field in the NJL model is significant because strong magnetic fields are produced in off-central heavy-ion collisions, which can create the conditions for observable QCD effects. Since strong magnetic fields are also present at the core of neutron stars, this model may illuminate more about QCD in astrophysical systems.

In this thesis, Chapters 2 and 3 will explore the concepts behind the QCD phase diagram and the two-flavor NJL model, respectively. Chapter 4 will list the parameters that are used and the assumptions that are made in the new calculations. Chapter 5 will demonstrate how a magnetic field explicitly changes the model seen in Chapters 3 and 4. In Chapter 6, new

results done using the modified model will be discussed.

2 The QCD Phase Diagram

2.1 Quarks and Gluons

Quarks are fundamental particles that possess intrinsic properties such as electric charge, color charge, mass and spin. There are six *flavors* of quarks: up (u), down (d), strange (s), charm (c), bottom (b), and top (t). For every quark, there exists a corresponding anti-quark, which can be denoted as $\bar{u}$, $\bar{d}$, $\bar{s}$, $\bar{c}$, $\bar{b}$, and $\bar{t}$, respectively. All quarks fall under the classification of elementary fermions of spin 1/2. The lightest quarks are u, d, and s and they are most likely to be found in quark matter. In this thesis, calculations are done only for the u and d quarks.

The *current* quark mass, the mass of a bare quark with no covering, of the u and d quarks are approximated to be $m_u \sim m_d \sim 5MeV$ [12]. On the other hand, the *constituent* quark mass is comprised of the current quark mass plus the mass-energy of the gluon particle field (the kinetic energy and the confining potential energy) that surrounds the quark. Thus, the constituent masses M_u and M_d are significantly larger than m_u and m_d by two orders of magnitude [13].

In addition to electric charge, $u : +\frac{2}{3}e$ and $d : -\frac{1}{3}e$, quarks also carry *color* charge. A quark can take on one of three color charges: red, green, and blue. These color charges denote an internal quantum state that quarks bear and hold no semblance to physical colors [13]. An anti-quark can take on one of three anti-colors: anti-red, anti-green, and anti-blue.

Quarks are the only fundamental particles that undergo all four fundamental interactions: electromagnetism, gravitation, strong interaction, and weak interaction. The strong interaction between quarks is mediated by elementary particles called *gluons*, which act as exchange particles (gauge bosons) between quarks. Similar to photons, gluons are spin-1 particles. However, gluons also possess color charge and thus partake in strong interaction as well as mediating it [13]. A possible consequence of gluons carrying color charge is the phenomenon

known as *confinement*, where a quark cannot be isolated and thus a free quark cannot be observed [13]. Quarks can only group together into colorless groups called *hadrons*. Hadrons can be divided into two families: *mesons* and *baryons*. Mesons are composed of one quark and one anti-quark and baryons are composed of three quarks.

The strength of quark-gluon interaction can be described by a coupling constant that depends on the energy scale of the system, which in turn depends on the baryon chemical potential. The *asymptotic freedom* feature of QCD details a property where quarks are nearly free from confinement when the chemical potential and/or the temperature become asymptotically large [13]. Thus, in the regions of high chemical potential or temperature, the interaction between quarks weakens.

2.2 QCD and Symmetries

The QCD Lagrangian is [14]

$$\mathcal{L} = \sum_{f}^{N_f} \bar{\psi}_f (i\gamma^\mu D_\mu - m_f)\psi_f - \frac{1}{4} G^a_{\mu\nu} G^a_{\mu\nu}, \tag{2.1}$$

where the covariant derivative acting on the quark fields ψ^a_f is

$$i\gamma^\mu D_\mu \psi = \gamma^\mu \left(i\partial_\mu + g A^a_\mu \frac{\lambda^a}{2} \right) \psi \tag{2.2}$$

and the field strength tensor is

$$G^a_{\mu\nu} = \partial_\mu A^a_\nu - \partial_\nu A^a_\mu + g f^{abc} A^b_\mu A^c_\nu. \tag{2.3}$$

The color index a transforms in the fundamental representation for fermions and in the adjoint representation for gluons A^a_μ. The flavor index f generally focuses on the three lightest quarks ($N_f = 3$).[1]

[1] In our calculations, only the u and d quarks will be considered.

The Lagrangian is invariant under local gauge transformations $U(x) \in SU(3)_C$

$$\psi(x) \to U(x)\psi(x), \qquad A(x) \to U(x)A_\mu U^\dagger(x) + iU(x)\partial_\mu U^\dagger(x), \tag{2.4}$$

where $A_\mu = A_\mu^a \frac{\lambda^a}{2}$ [14]. It is apparent that the interactions are flavor-independent. If the quark masses are equal, then the Lagrangian is invariant under any flavor rotations of the quark fields $\psi_f \to V_{fg}\psi_g$, where $V \in SU(3)$. In strong interaction, this is known as flavor (isospin) symmetry. *Isospin* is a dimensionless quantity that uses similar mathematics as those used to describe spin. Isospin symmetry arises from the nearly identical masses of the u and d quarks. The total isospin of both quarks is $I = 1/2$, but the isospin component I_3 for the u and d quarks are assigned to be $I_3 = 1/2$ and $I_3 = -1/2$, respectively. All other quarks have $I = 0$. Although isospin symmetry is slightly broken, $SU(3)$ symmetry does not hold as well due to the much higher mass of the s quark.[2] If the quark masses are zero, then there is a larger flavor symmetry in play. If we define the left and right-handed fields as

$$\psi_{L,R} = \frac{1}{2}(1 \pm \gamma_5)\gamma, \tag{2.5}$$

then the Lagrangian of the fermions can be written as

$$\mathcal{L} = \bar{\psi}_L(i\gamma^\mu D_\mu)\psi_L + \bar{\psi}_R(i\gamma^\mu D_\mu)\psi_R + \bar{\psi}_L m\psi_R + \bar{\psi}_R m\psi_L, \tag{2.6}$$

where $m = \begin{pmatrix} m_u & 0 & 0 \\ 0 & m_d & 0 \\ 0 & 0 & m_s \end{pmatrix}$. In this case, there is no coupling between the left and right-handed fields when the quark masses are zero. Therefore, the Lagrangian is invariant under independent flavor transformations of the left and right-handed fields [14]

$$\psi_{L,f} \to L_{fg}\psi_{L,g}, \qquad \psi_{R,f} \to R_{fg}\psi_{R,g}, \tag{2.7}$$

[2] $m_s \sim 100MeV$

where $(L, R) \in SU(3)_L \times SU(3)_R$. Even in the case where the masses are not zero, QCD has an approximate chiral symmetry due to the small values of m_u, m_d, and m_s.

In addition, the Lagrangian has two $U(1)$ symmetries [14]

$$U(1)_B : \qquad \psi_L \to e^{i\phi}\psi_L, \qquad \psi_R \to e^{i\phi}\psi_R \tag{2.8}$$

$$U(1)_A : \qquad \psi_L \to e^{i\alpha}\psi_L, \qquad \psi_R \to e^{-i\alpha}\psi_R. \tag{2.9}$$

The $U(1)_B$ symmetry holds even in the case of $m_u \neq 0$ and $m_d \neq 0$. However, the axial $U(1)_A$ symmetry only holds at the classical level and breaks at the quantum level.

Without the presence of a baryon chemical potential in QCD, both space-time and $U(1)$ symmetries cannot be broken. Hence, the phases of QCD are controlled by the attainment of the chiral symmetry $SU(3)_L \times SU(3)_R$. However, in the presence of a baryon chemical potential, both space-time and $U(1)$ symmetries can be broken [14].

2.3 Universal Properties of the Tricritical Point

True to its name, the TCP marks a point where three coexisting phases are reduced to the same phase simultaneously. In QCD, it is necessary to add the quark mass m to the parameter space since it explicitly breaks chiral symmetry. In a three-dimensional parameter space, there are two surfaces of first-order transitions that arise from the first-order line at $m = 0$. These two surfaces are symmetric with respect to $m \to -m$ reflection. At $m \neq 0$, a low chemical potential phase and a high chemical potential phase coexist on these surfaces since chiral symmetry is explicitly broken. Without chiral symmetry, there is no symmetry to separate these two phases. Hence, these surfaces can possess an edge, which is a curve that originates from the TCP. Thus, the first-order phase transition curve contains three phases coexisting: the high-T/high-μ phase, low-μ/low-T with $m > 0$ phase, and low-μ/low-

T with $m < 0$ phase.[3] Since chiral symmetry can only be exact on the $m = 0$ plane, a phase transition between the low-T and the high-T phases must be at this plane [6]. The second-order phase transition curve in conjunction with the first-order phase transition curve make up a phase boundary for the $m = 0$ plane.

Behavior near the TCP can be described by expanding the thermodynamic potential in a power series in the order parameter $\phi \sim \langle\bar{\psi}\psi\rangle$ by way of Landau theory [15]. In the $m = 0$ plane,

$$\Omega_{eff} = \Omega_0(T,\mu) + a(T,\mu)\phi^2 + b(T,\mu)\phi^4 + c(T,\mu)\phi^6 \tag{2.10}$$

where the ϕ^6 term is necessary for the three minima to characterize the three coexisting phases and $c > 0$ for stability. When $b > 0$, the second-order phase transition curve is found at $a = 0$. When $b < 0$, the first-order phase transition curve is found at $a > 0$. Therefore, the point at which $a = b = 0$ can be identified as the TCP [6].

[3]This is the same as two low-μ/low-T phases with opposite signs for $\langle\bar{\psi}\psi\rangle$.

3 Two-Flavor NJL Model

3.1 Origin/Formulation of the Model

The NJL model is an effective, chiral model of nucleons and mesons composed of interacting fermions. It was formulated to describe the dynamical mass generation of hadrons as a parallel to the construction of Cooper pairs from electrons in the Bardeen-Cooper-Schrieffer (BCS) theory of superconductivity [16]. At the time, quarks had not been discovered yet. Thus, the model does not include gluons and color charge. However, the model is now generally used as a low-energy approximation of QCD, particularly to analyze the restoration of chiral symmetry.

The Lagrangian of the NJL model for two quark flavors is [12]

$$\mathcal{L} = \bar{\psi}(i\gamma^\mu\partial_\mu - m)\psi + G_S[(\bar{\psi}\psi)^2 + (\bar{\psi}i\boldsymbol{\tau}\gamma_5\psi)^2] - G_V^{(S)}(\bar{\psi}\gamma_\mu\psi)^2$$

$$-G_V^{(V)}[(\bar{\psi}\boldsymbol{\tau}\gamma_\mu\psi)^2 + (\bar{\psi}\boldsymbol{\tau}\gamma_\mu\gamma_5\psi)^2] + \bar{\psi}\mu\gamma_0\psi; \tag{3.1}$$

the quark and anti-quark fields ψ, $\bar{\psi}$, the current quark mass m, and the chemical potential μ are defined as

$$\psi = \begin{pmatrix} \psi_u \\ \psi_d \end{pmatrix}, \quad \bar{\psi} = \begin{pmatrix} \bar{\psi}_u \\ \bar{\psi}_d \end{pmatrix}, \quad m = \begin{pmatrix} m_u & 0 \\ 0 & m_d \end{pmatrix}, \quad \mu = \begin{pmatrix} \mu_u & 0 \\ 0 & \mu_d \end{pmatrix} \tag{3.2}$$

and $\boldsymbol{\tau}$ are the Pauli matrices in isospin space. The first term of Eq. (3.1) is the free (Dirac) part for the quark fields ψ and $\bar{\psi}$ with mass m. The strength of the interaction in the scalar and vector channels is parametrized by the dimensionful[4] scalar (G_S), vector-isoscalar ($G_V^{(S)}$), and vector-isovector ($G_V^{(V)}$) coupling constants [12]. *Isoscalar* denotes a scalar trans-

[4]Dimensions of coupling constants: $[G_S] = \left[G_V^{(S)}\right] = \left[G_V^{(V)}\right] = -2$

formation[5] and *isovector* denotes a vector transformation[6] of a field under the $SU(2)$ group of isospin. The last term of Eq. (3.1) contains the chemical potential μ, which controls the constraints imposed by the conservation of the net quark number of different flavors. This term can be rewritten in terms of the quark chemical potential $\mu_q = \frac{1}{2}(\mu_u + \mu_d)$ and the isovector chemical potential $\mu_I = \frac{1}{2}(\mu_u - \mu_d)$ as [12]

$$\mathcal{L}_\mu = \bar{\psi}\mu\gamma_0\psi = \mu_q\psi^\dagger\psi + \mu_I\psi^\dagger\tau_3\psi. \tag{3.3}$$

In addition to m and the three coupling constants, the model requires another parameter known as the *momentum cutoff* Λ. Λ regularizes the model using a sharp cutoff for the divergent integrals. In vacuum, Λ and G_S are fixed by requiring that empirical values of the pion decay constant f_π and the pion mass m_π are reproduced. The other two coupling constants are also fixed based on empirical values of a quark model for nucleons [12].

Since QCD interactions are flavor-independent and m_u and m_d are approximated to be equal, there is an $N_f = 2$ degeneracy in flavor space. Thus, Eq. (3.1) has isospin symmetry $SU(2)_f$. Additionally, all interactions are color-independent and this leads to an $N_c = 3$ degeneracy in color space [16].

Chiral symmetry is explicitly broken when $m \neq 0$, which can occur in the $\bar{\psi}m\psi$ term of Eq. (3.1). In the chiral limit $m = 0$, the spontaneously broken chiral symmetry is restored [16].

3.2 Finite T and μ

At finite T and non-zero quark and isovector chemical potentials, the thermodynamics of the model is acquired by implementing the mean field approximation to Eq. (3.1). In the mean field approximation, the interaction terms in Eq. (3.1) are linearized in the presence

[5] $I = 0$ and $I_3 = 0$. This is a singlet state.
[6] $I = 1$ and $I_3 = -1, 0, 1$. This is a triplet state.

of three non-vanishing condensates: the scalar condensate $\langle\bar{\psi}\psi\rangle$, the quark number density $\langle\bar{\psi}\gamma_0\psi\rangle$, and the isovector density $\langle\bar{\psi}\tau_3\gamma_0\psi\rangle$,. The interaction terms are linearized to [17]

$$(\bar{\psi}\psi)^2 \simeq 2\langle\bar{\psi}\psi\rangle\bar{\psi}\psi - (\langle\bar{\psi}\psi\rangle)^2, \qquad (\bar{\psi}\gamma_\mu\psi)^2 \simeq 2\langle\bar{\psi}\gamma_0\psi\rangle\bar{\psi}\gamma_0\psi - (\langle\bar{\psi}\gamma_0\psi\rangle)^2,$$

$$(\bar{\psi}\tau\gamma_\mu\psi)^2 \simeq 2\langle\bar{\psi}\tau_3\gamma_0\psi\rangle\bar{\psi}\gamma_0\psi - (\langle\bar{\psi}\tau_3\gamma_0\psi\rangle)^2. \tag{3.4}$$

The quadratic terms in the fluctuations are neglected. Moreover, terms in channels without condensates such as $(\bar{\psi}i\boldsymbol{\tau}\gamma_5\psi)^2$ or spatial components in the vector channel are also neglected. Thus, in this approximation, Eq. (3.1) turns into

$$\mathcal{L}_{\text{effective}} = \bar{\psi}(i\gamma^\mu\partial_\mu - M + \tilde{\mu}\gamma_0)\psi - \frac{1}{4G_S}\text{tr}((M-m)^2) + \frac{1}{4G_V^{(S)}}(\tilde{\mu}_q - \mu_q)^2 + \frac{1}{4G_V^{(V)}}(\tilde{\mu}_I - \mu_I)^2; \tag{3.5}$$

the *dynamical mass* M is defined as

$$M = \begin{pmatrix} M_u & 0 \\ 0 & M_d \end{pmatrix} = m - 2G_S\langle\bar{\psi}\psi\rangle, \tag{3.6}$$

and the trace is taken in flavor space. The shifted chemical potential $\tilde{\mu}$ is given by

$$\tilde{\mu} = \tilde{\mu}_q + \tilde{\mu}_I\tau_3, \tag{3.7}$$

in which [17]

$$\tilde{\mu}_q = \mu_q - 2G_V^{(S)}\langle\bar{\psi}\gamma_0\psi\rangle \tag{3.8}$$

$$\tilde{\mu}_I = \mu_I - 2G_V^{(V)}\langle\bar{\psi}\tau_3\gamma_0\psi\rangle. \tag{3.9}$$

In the mean field approximation, the partition function $Z(T, \mu_q, \mu_I, V)$ can be obtained from

Eq. (3.5).[7] Then, the thermodynamic potential density $\omega = -\frac{T}{V}\ln(Z)$ is given by [17]

$$\omega(T,\mu;M,\tilde{\mu}) = \sum_{f=u,d}\omega_f(T,\mu;M_f,\tilde{\mu}_f) + \frac{1}{4G_S}\mathrm{tr}((M-m)^2)$$

$$-\frac{1}{4G_V^{(S)}}(\tilde{\mu}_q-\mu_q)^2 - \frac{1}{4G_V^{(V)}}(\tilde{\mu}_I-\mu_I)^2 \tag{3.10}$$

where

$$\omega_f(T,\mu;M_f,\tilde{\mu}_f) = -2N_c\int\frac{d^3p}{(2\pi)^3}[E_f(\boldsymbol{p}) - T\ln(1-n_f^{(+)}(\boldsymbol{p},T,\tilde{\mu}_f))$$

$$-T\ln(1-n_f^{(-)}(\boldsymbol{p},T,\tilde{\mu}_f))]. \tag{3.11}$$

The dispersion relation in Eq. (3.10) is $E_f(\boldsymbol{p}) = \sqrt{\boldsymbol{p}^2+M_f^2}$ and $n_f^{(\pm)}$ are the distribution functions for the particle $(+)$ and antiparticle $(-)$ states

$$n_f^{(\pm)}(\boldsymbol{p},T,\tilde{\mu}_f) = \frac{1}{1+\exp\left(\dfrac{E_f(\boldsymbol{p})\mp\tilde{\mu}_f}{T}\right)}. \tag{3.12}$$

The scalar condensate in Eq. (3.6), the quark number density in Eq. (3.8), and the isovector density in Eq. (3.9) can be calculated by extremizing Eq. (3.10) such that

$$\frac{\partial\omega}{\partial M} = \frac{\partial\omega}{\partial\tilde{\mu}_q} = \frac{\partial\omega}{\partial\tilde{\mu}_I} = 0. \tag{3.13}$$

Applying the first stationary condition in Eq. (3.13) gives the mass gap equation

$$M_f = m_f + 4G_SN_c\sum_{f=u,d}\int\frac{d^3p}{(2\pi)^3}\frac{M_f}{E_f}\left[1-n_f^{(+)}(\boldsymbol{p},T,\tilde{\mu}_f)) - n_f^{(-)}(\boldsymbol{p},T,\tilde{\mu}_f)\right]. \tag{3.14}$$

The other two stationary conditions in Eq. (3.13) imply

$$\mu_q = \tilde{\mu}_q + 4G_V^{(S)}N_c\sum_{f=u,d}\int\frac{d^3p}{(2\pi)^3}\left[n^{(+)}(\boldsymbol{p},T,\tilde{\mu}_f)) - n_f^{(-)}(\boldsymbol{p},T,\tilde{\mu}_f)\right] \tag{3.15}$$

[7] V is the volume of the system.

$$\mu_I = \tilde{\mu}_I + 4G_V^{(V)} N_c \sum_{f=u,d} \int \frac{d^3p}{(2\pi)^3} \left[(n_u^{(+)}(\boldsymbol{p}, T, \tilde{\mu}_f)) - n_u^{(-)}(\boldsymbol{p}, T, \tilde{\mu}_f)) - (u \to d) \right]. \quad (3.16)$$

The phase boundary between the chirally broken and the symmetric phases can be located by finding the onset of chiral symmetry restoration at $M = 0$ when approaching from the broken phase. At the second order phase transition, Eq. (3.14) has a nontrivial solution at $M = 0$ such that [12]

$$1 = 4G_S N_c \sum_{f=u,d} \int \frac{d^3p}{(2\pi)^3} \frac{1}{p} \left[1 - n_f^{(+)}(\boldsymbol{p}, T, \tilde{\mu}_f)) - n_f^{(-)}(\boldsymbol{p}, T, \tilde{\mu}_f) \right] \quad (3.17)$$

is satisfied.[8] Thus, the position of the phase boundary in the (T, μ)-plane is calculated by satisfying Eq. (3.17).

In the chiral limit $m = 0$, the order of the chiral transition is expected to change from second order at low chemical potentials to first order at high chemical potentials. Therefore, somewhere along the phase boundary, a TCP is expected when the order of the phase transition changes. Near the phase boundary, the thermodynamic potential density in Eq. (3.10) can be expanded in a power series using the order parameter M:

$$\omega(T, \mu; M, \tilde{\mu}) = \omega_0 + \frac{1}{2} a M^2 + \frac{1}{4} b M^4 + \frac{1}{6} c M^6. \quad (3.18)$$

As discussed earlier[9], the TCP can be determined by finding the point that satisfies $a = b = 0$.

3.3 Advantages and Disadvantages of the Model

The NJL model does not exhibit confinement and consequently the hadronic degrees of freedom are missing from the model. In addition, the model does not have gluon degrees of freedom. In QCD, gluons play a significant role in the thermodynamics of the chirally

[8] $m_f = 0$ and M_f is canceled from both sides of Eq. (3.14). Then M_f is evaluated at 0, giving $E_f = p$.
[9] Landau theory in Section 2.4

symmetric/deconfined phase. Lastly, the model is strongly dependent on the momentum cutoff Λ.

Despite these disadvantages, the model reproduces the entire structure expected in the QCD phase diagram. In the chiral limit, the NJL model shows a phase boundary, where the spontaneously broken chiral symmetry is restored. At small chemical potentials, the phase transition is second order and at large chemical potentials and appropriate coupling constants, the phase transition is first order. Accordingly, the model can be used to study the universal properties of the chiral phase transition in the (T, μ)-plane.

4 Charged Medium

The model discussed in Chapter 3 has a degeneracy of $N_f = 2$ in flavor space. Hence, there is a summation term $\sum_{f=u,d}$ in Eqs. (3.10), (3.14)-(3.17) in order to include this degeneracy. This sum in flavor space term is taken into account when values of Λ and G_S are fixed.[10] Table 1 shows three sets of fixed parameters calculated for this model.

	Λ(MeV)	$G_S\Lambda^2$
Set A	664.3	2.060
Set B	797.2	1.935
Set C	995.5	1.829

Table 1: Set of momentum cutoff Λ and scalar coupling constant G_S for Chapter 3 model

In our calculations, the isovector chemical potential μ_I is chosen to be zero, which implies that $\mu_u = \mu_d$. Thus, Eqs. (3.7)-(3.9) simplify to $\tilde{\mu} = \tilde{\mu}_q = \tilde{\mu}_u = \tilde{\mu}_d$. A system where the number of u and d quarks are equal is a charged system. Since u and d quarks have different electric charges and $\mu_u = \mu_d$ denotes that they have the same Fermi surface, the net charge of the system cannot be zero. In addition, our model does not have a sum in flavor space and all calculations are done in the chiral limit $m = 0$. Thus, our thermodynamic potential density is

$$\omega(T, \mu; M, \tilde{\mu}) = \omega_f(T, \mu; M_f, \tilde{\mu}_f) + \frac{1}{4G_S}\mathrm{tr}(M^2) - \frac{1}{4G_V^{(S)}}(\tilde{\mu}_q - \mu_q)^2. \tag{4.1}$$

The stationary conditions $\dfrac{\partial\omega}{\partial M} = \dfrac{\partial\omega}{\partial\tilde{\mu}} = 0$ would give the mass gap equation

$$M_f = 4G_S N_c \int \frac{d^3p}{(2\pi)^3}\frac{M_f}{E_f}\left[1 - n_f^{(+)}(\boldsymbol{p}, T, \tilde{\mu}_f)) - n_f^{(-)}(\boldsymbol{p}, T, \tilde{\mu}_f)\right] \tag{4.2}$$

[10] Empirical values of the pion decay constant f_π, the pion mass m_π, and critical temperature $T_C = 177$MeV at $\mu_q = 0$ are reproduced.

and the chemical potential

$$\mu = \mu_u = \mu_d = \tilde{\mu} + 4G_V^{(S)} N_c \int \frac{d^3p}{(2\pi)^3} \left[n^{(+)}(\boldsymbol{p}, T, \tilde{\mu}_f)) - n_f^{(-)}(\boldsymbol{p}, T, \tilde{\mu}_f) \right]. \tag{4.3}$$

At the second order phase transition, Eq. (4.2) has a nontrivial solution at $M = 0$ such that

$$1 = 4G_S N_c \int \frac{d^3p}{(2\pi)^3} \frac{1}{p} \left[1 - n_f^{(+)}(\boldsymbol{p}, T, \tilde{\mu}_f)) - n_f^{(-)}(\boldsymbol{p}, T, \tilde{\mu}_f) \right] \tag{4.4}$$

is satisfied, which is the onset of chiral symmetry restoration.

	Λ(MeV)	$G_S\Lambda^2$
Set A	664.3	4.124
Set B	797.2	3.871
Set C	995.5	3.659

Table 2: Set of momentum cutoff Λ and scalar coupling constant G_S for our model

Using the same three values of Λ in Table 1, Table 2 shows our three sets of fixed parameters calculated for our model. Evidently, the values of $G_S\Lambda^2$ in Table 2 are twice the values in Table 1 since there is no sum in flavor space in our model.

5 Two-Flavor NJL Model with Magnetic Field

When a magnetic field is added to the NJL model, the $i\gamma^\mu\partial_\mu$ term in the Lagrangian in Eqs. (3.1) and (3.5) transforms as

$$i\gamma^\mu\partial_\mu \to i\gamma^\mu D_\mu = (i\gamma^\mu\partial_\mu - qA_\mu), \tag{5.1}$$

where $q = \begin{pmatrix} q_u & 0 \\ 0 & q_d \end{pmatrix}$. With the Lagrangian of the system changed, the thermodynamic potential density must also change. In the presence of an external magnetic field along the z-direction, the spatial momentum transforms as [18]

$$\int_{-\infty}^{\infty}\frac{d^3p}{(2\pi)^3} \to \frac{|q_fB|}{2\pi}\sum_{l=0}^{\infty}\left(1-\frac{1}{2}\delta_{l0}\right)\int_{-\infty}^{\infty}\frac{dp_3}{2\pi}. \tag{5.2}$$

The spatial momentum now depends on the Landau level l, and the integration in the two transverse momentum components is replaced by a sum in the Landau levels. In Eq. (5.2), q_f is the electric charge of the quark and B is the strength of the magnetic field. Using the change seen in Eq. (5.2), Eq. (3.11) and the dispersion relation can now be written as

$$\omega_f = -2N_c\frac{|q_fB|}{2\pi}\sum_{l=0}^{\infty}(1-\tfrac{1}{2}\delta_{l0})\int_{-\infty}^{\infty}\frac{dp_3}{2\pi}\left[E_f - T\ln(1-n_f^{(+)}) - T\ln(1-n_f^{(-)})\right], \tag{5.3}$$

$$E_f = \sqrt{p_3^2 + 2|q_fB|l + M_f^2}. \tag{5.4}$$

Similar to the general NJL model, the momentum is also limited by the momentum cutoff. Thus, the limits of integration and summation follow such that the momentum $\sqrt{p_3^2+2|q_fB|l}$ always satisfies $\sqrt{p_3^2+2|q_fB|l} \leq \Lambda$. As discussed in Chapter 4, our model does not include a sum in flavor space for the thermodynamic potential density. In the presence of a magnetic field, the model has two decoupled mass gap equations due to the two different electric charges for the u and d quarks. For $\dfrac{\partial\omega}{\partial M_u} = 0$, the resulting mass gap equation for the u

quark is

$$M_u = 4G_S N_c \frac{|q_u B|}{2\pi} \sum_{l=0}^{\left[\frac{\Lambda^2}{2|q_u B|}\right]} (2-\delta_{l0}) \int_0^{\sqrt{\Lambda^2 - 2|q_u B|l}} \frac{dp_3}{2\pi} \frac{M_u}{\sqrt{p_3^2 + 2|q_u B|l + M_u^2}}$$

$$\times \left[1 - \frac{1}{1+\exp\left(\frac{\sqrt{p_3^2+2|q_u B|l+M_u^2}-\tilde{\mu}}{T}\right)} - \frac{1}{1+\exp\left(\frac{\sqrt{p_3^2+2|q_u B|l+M_u^2}+\tilde{\mu}}{T}\right)} \right] \tag{5.5}$$

and for $\dfrac{\partial \omega}{\partial M_d} = 0$, the resulting mass equation for the d quark is

$$M_d = 4G_S N_c \frac{|q_d B|}{2\pi} \sum_{l=0}^{\left[\frac{\Lambda^2}{2|q_d B|}\right]} (2-\delta_{l0}) \int_0^{\sqrt{\Lambda^2 - 2|q_d B|l}} \frac{dp_3}{2\pi} \frac{M_d}{\sqrt{p_3^2 + 2|q_d B|l + M_d^2}}$$

$$\times \left[1 - \frac{1}{1+\exp\left(\frac{\sqrt{p_3^2+2|q_d B|l+M_d^2}-\tilde{\mu}}{T}\right)} - \frac{1}{1+\exp\left(\frac{\sqrt{p_3^2+2|q_d B|l+M_d^2}+\tilde{\mu}}{T}\right)} \right]. \tag{5.6}$$

Additionally, for $\dfrac{\partial \omega}{\partial \tilde{\mu}} = 0$

$$\mu = \tilde{\mu} + 4G_V^{(S)} N_c \frac{|q_f B|}{2\pi} \sum_{l=0}^{\left[\frac{\Lambda^2}{2|q_f B|}\right]} (2-\delta_{l0}) \int_0^{\sqrt{\Lambda^2 - 2|q_f B|l}} \frac{dp_3}{2\pi}$$

$$\times \left[\frac{1}{1+\exp\left(\frac{\sqrt{p_3^2+2|q_f B|l+M_f^2}-\tilde{\mu}}{T}\right)} - \frac{1}{1+\exp\left(\frac{\sqrt{p_3^2+2|q_f B|l+M_f^2}+\tilde{\mu}}{T}\right)} \right]. \tag{5.7}$$

In consequence of the two separate mass gap equations, there are two different phase boundaries in the chiral limit. The solution of Eq. (5.5) at $M_u = 0$ gives a phase boundary that satisfies

$$1 = \frac{2G_s N_c q_u B}{\pi^2} \sum_{l=0}^{\left[\frac{\Lambda^2}{2|q_u B|}\right]} (1 - \tfrac{1}{2}\delta_{l0}) \int_0^{\sqrt{\Lambda^2 - 2|q_u B|l}} \frac{dp_3}{\sqrt{p_3^2 + 2|q_u B l|}}$$

$$\times \left[1 - \frac{1}{1 + \exp\left(\dfrac{\sqrt{p_3^2 + |2q_u B l|} - \tilde{\mu}}{T} \right)} - \frac{1}{1 + \exp\left(\dfrac{\sqrt{p_3^2 + 2|q_u B|l} + \tilde{\mu}}{T} \right)} \right] \tag{5.8}$$

and the solution of Eq. (5.6) at $M_d = 0$ gives a phase boundary that satisfies

$$1 = \frac{2G_s N_c q_d B}{\pi^2} \sum_{l=0}^{\left[\frac{\Lambda^2}{2|q_d B|}\right]} (1 - \tfrac{1}{2}\delta_{l0}) \int_0^{\sqrt{\Lambda^2 - 2|q_d B|l}} \frac{dp_3}{\sqrt{p_3^2 + 2|q_d B l|}}$$

$$\times \left[1 - \frac{1}{1 + \exp\left(\dfrac{\sqrt{p_3^2 + |2q_d B l|} - \tilde{\mu}}{T} \right)} - \frac{1}{1 + \exp\left(\dfrac{\sqrt{p_3^2 + 2|q_d B|l} + \tilde{\mu}}{T} \right)} \right]. \tag{5.9}$$

The approach to finding the TCP for each phase boundary is similar to the discussion in Sections 2.3 and 3.2. To find the TCP for the phase boundaries in Eqs. (5.8) and (5.9), ω is expanded in a power series using the order parameters M_u and M_d respectively. Each TCP is located at $a = b = 0$.

6 Results and Discussion

The following results are done using the two-flavor NJL model seen in Chapter 4 and the model in the presence of a magnetic field seen in Chapter 5. The model is implemented using a combination of Mathematica and my own C programs (see Appendix).

Before introducing a magnetic field, the phase boundary between the chirally broken and the symmetric phases is first calculated using Eq. (4.4). The TCP between the second order transition and the first order transition of this phase boundary is determined using Eq. (3.18). Next, a magnetic field is introduced and two phase boundaries are produced for the u and d quarks using Eqs. (5.8) and (5.9), respectively. Figures 6.1-6.3 use the fixed parameter values from Set A of Table 2.

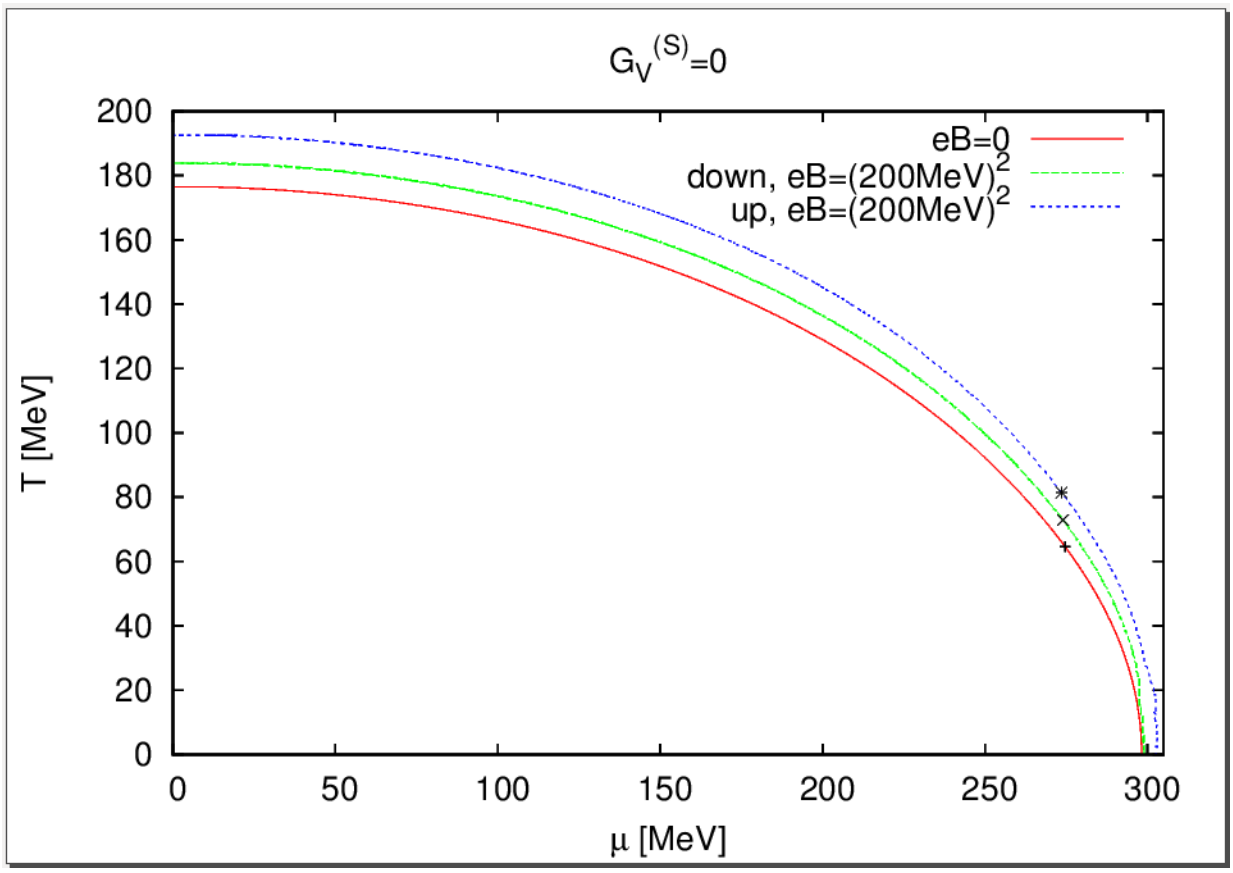

Figure 6.1: Phase boundary at eB=$(200\text{MeV})^2$ and at zero magnetic field

Figure 6.1 shows the phase boundary at zero magnetic field, $eB = (200\text{MeV})^2$ for the u quark, and $eB = (200\text{MeV})^2$ for the d quark at the same coupling constants G_S and $G_V^{(S)} = 0$. The TCP for the phase boundary at zero magnetic field is $(274.6, 64.6)$MeV, $(274, 83.15)$MeV at $eB = (200\text{MeV})^2$ for the d quark, and $(273.5, 81.5)$MeV at $eB = (200\text{MeV})^2$ for the u quark. The phase boundary and TCP for the u and d quarks at the same magnetic field are slightly sensitive to the charge of the quark since the expression of energy of the quark in Eq. (5.4) depends on the charge and the Landau level being summed. This can be seen in the slightly higher curve of the phase boundary of the u quark. The phase boundary for u quark and the phase boundary for the d quark are both shifted to higher temperatures and chemical potentials compared to the phase boundary at zero magnetic field.

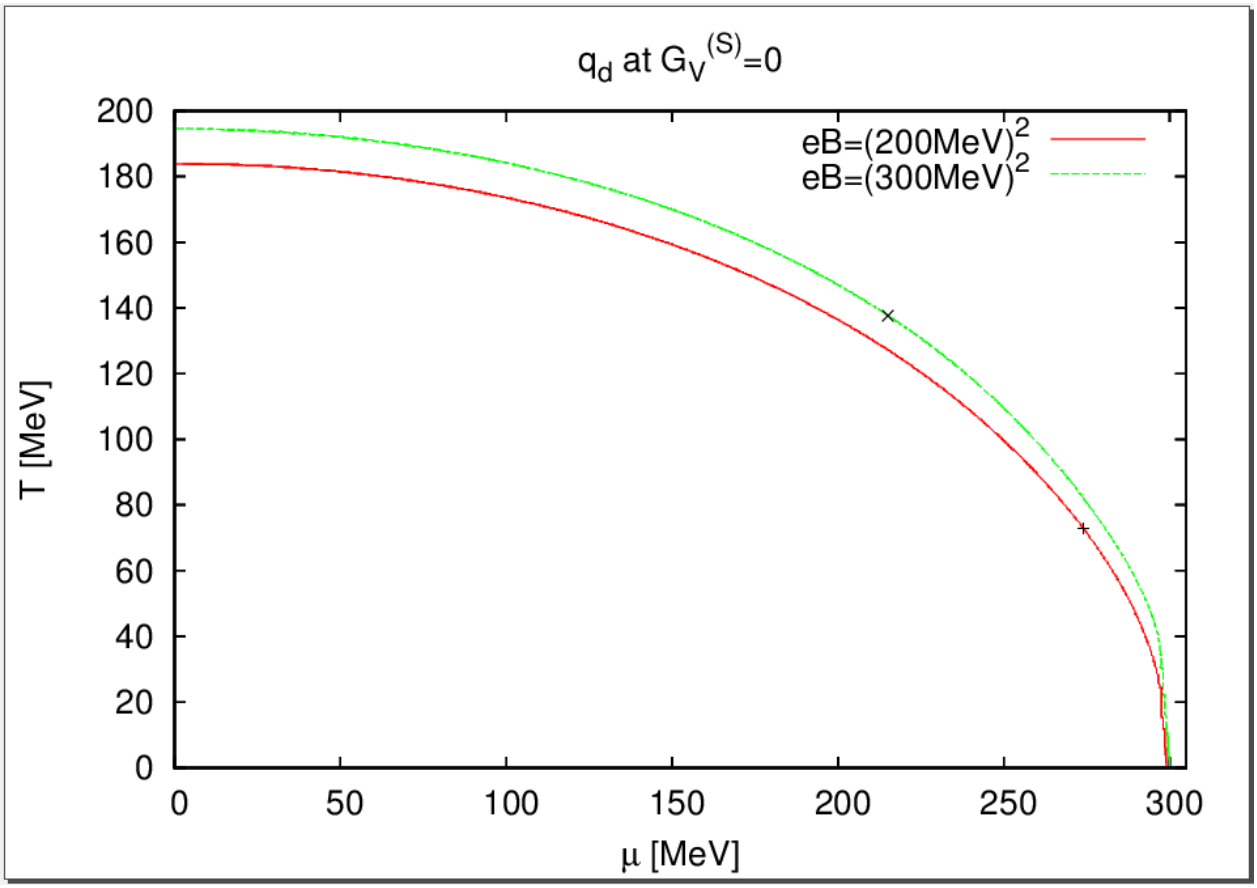

Figure 6.2: Phase boundary for down quark at varying magnetic fields

Figure 6.2 shows the phase boundary for the d quark at two different magnetic fields and at the same coupling constants G_s and $G_V^{(S)} = 0$. The TCP at $eB = (200\text{MeV})^2$ is $(274, 83.15)$MeV and at $eB = (300\text{MeV})^2$ is $(215, 137.65)$MeV. As the magnetic field increases, the phase boundary shifts to higher temperatures and chemical potentials. In addition, the change in the location of the TCP demonstrates that the phase boundary favors the first order phase transition. The second order phase transition is in the region of small chemical potentials before the phase boundary has reached the TCP and the first order phase transition is the latter part of the phase boundary after the TCP. It is evident that as the magnetic field increases, the phase boundary remains in second order phase transition for a smaller range of chemical potentials. The change to first order phase transition occurs at a smaller chemical potential.

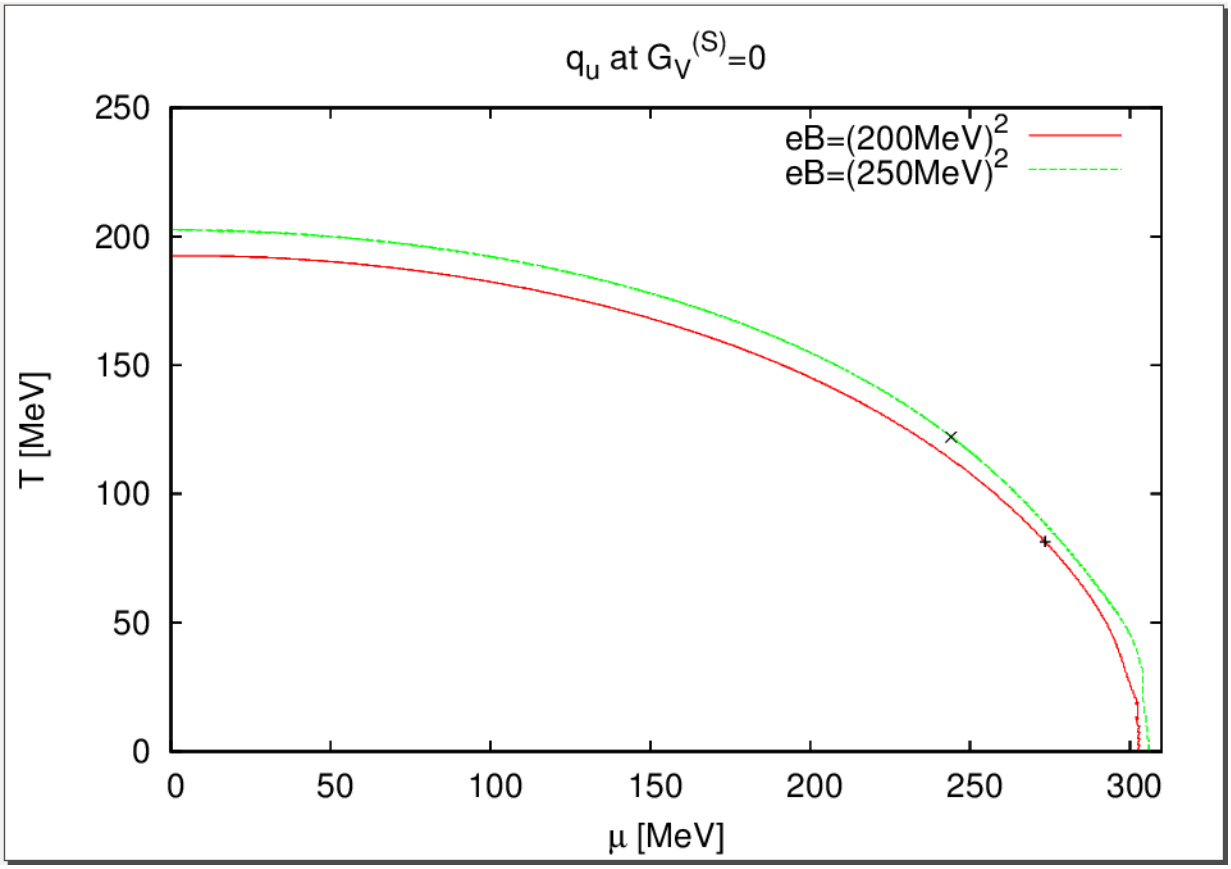

Figure 6.3: Phase boundary for up quark at varying magnetic fields

Figure 6.3 shows the phase boundary for the u quark at two different magnetic fields and at the same coupling constants G_S and $G_V^{(S)} = 0$. The TCP at $eB = (200\text{MeV})^2$ is $(273.5, 81.5)$MeV and at $eB = (250\text{MeV})^2$ is $(244, 122.15)$MeV. Similar to the d quark, the phase boundary of the u quark shifts to higher temperatures and chemical potentials as the magnetic field increases. Moreover, the change in the location of the TCP displays that the phase boundary exhibits a favoring of the first order phase transition for increasing magnetic fields.

Since time did not permit calculations for the phase boundary at different values of $G_V^{(S)}$ from Table 2, the next three figures will show the phase boundaries and their respective TCP at different values of $G_V^{(S)}$ from Set A of Table 1. As mentioned earlier, Table 1 is a list of fixed parameters calculated from a model that includes a sum in flavor. On the other hand, Figures 6.1-6.3 use parameter values from Table 2, which does not include this sum.

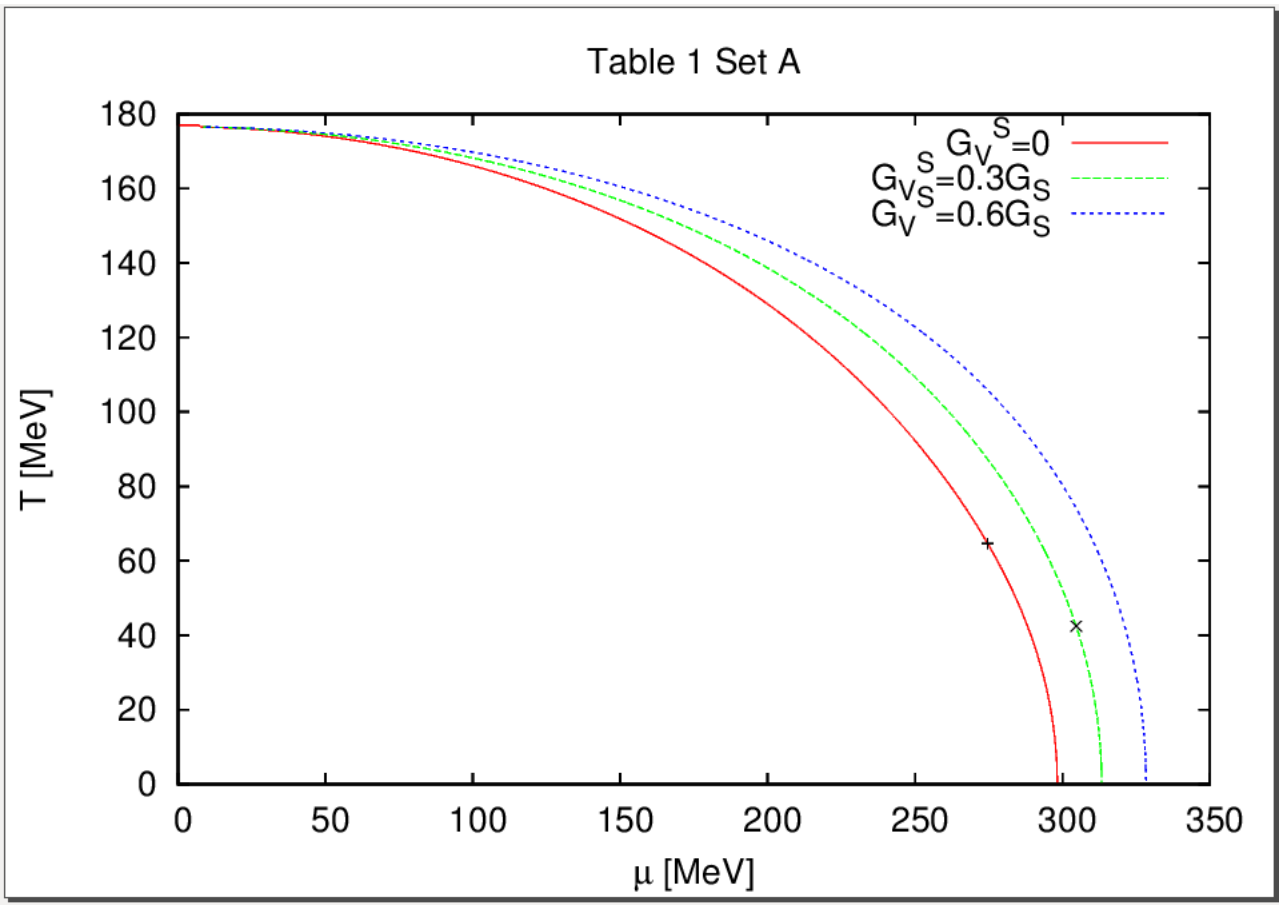

Figure 6.4: Phase boundary at zero magnetic field for different $G_V^{(S)}$

Figure 6.4 shows the phase boundary at zero magnetic field for three different values of $G_V^{(S)}$. The TCP for $G_V^{(S)}$=0 is $(274.6, 64.6)$MeV, $G_V^{(S)} = 0.3G_S$ is $(304.6, 42.4)$MeV, and there is no TCP for $G_V^{(S)} = 0.6G_S$. Eq. (3.15) indicates that the critical temperature at which $\mu = 0$ is the same for all three curves. It is clear that the bigger the $G_V^{(S)}$ coupling constant, the more the chemical potentials shift to higher values. The phase boundary favors the second order phase transition, as seen in the change of the location of the TCP, as $G_V^{(S)}$ increases. The phase boundary remains in second order phase transition for a larger range of chemical potentials for increasing $G_V^{(S)}$.

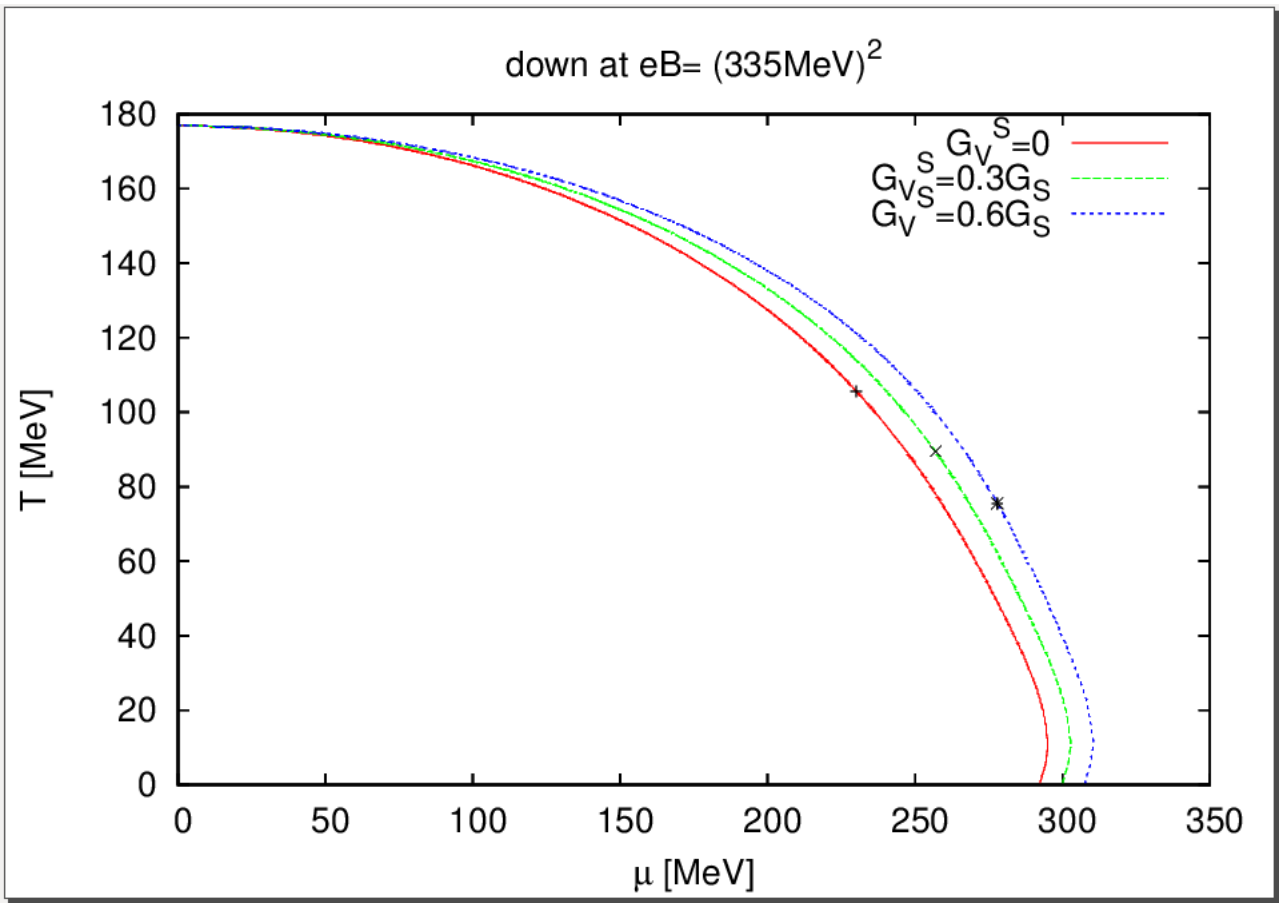

Figure 6.5: Phase boundary for down quark at eB=(335MeV)^2 for different $G_V^{(S)}$

Figure 6.5 shows the phase boundary for the d quark at the same magnetic field $eB = (335\text{MeV})^2$ and the same coupling constant G_S. However, the effect of changing the coupling constant $G_V^{(S)}$ is studied here for three different values. The TCP at $G_V^{(S)} = 0$ is $(230, 105.5)$MeV, at $G_V^{(S)} = 0.3G_S$ is $(256.9, 89.5)$MeV, and at $G_V^{(S)} = 0.6G_S$ is $(277.9, 75.5)$MeV. Eqs. (3.15) and (5.7) indicate that the vector-isoscalar coupling constant $G_V^{(S)}$ affects the shift in chemical potentials. Thus, the critical temperature at which $\mu = 0$ is the same for all three curves. It is clear that the bigger the $G_V^{(S)}$ coupling constant, the more the chemical potentials shift to higher values. The phase boundary also favors the second order phase transition, as seen in the change in location of the TCP, at a constant magnetic field and increasing $G_V^{(S)}$.

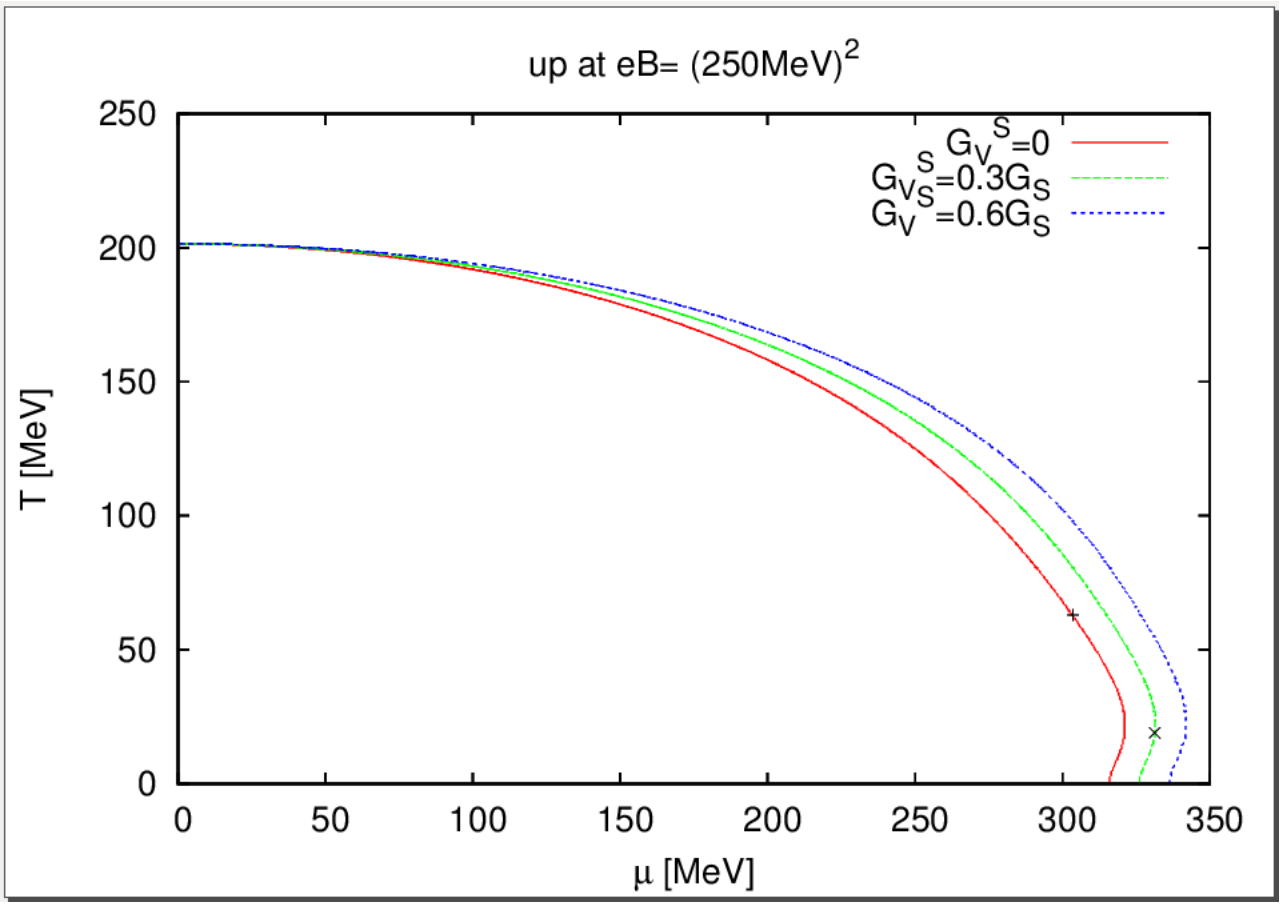

Figure 6.6: Phase boundary for up quark at eB=(250MeV)^2 for different $G_V^{(S)}$

Figure 6.6 shows the phase boundary for the u quark at the same magnetic field $eB = (250MeV)^2$ and the same coupling constant G_S. The TCP at $G_V^{(S)} = 0$ is $(302, 65)$MeV and at $G_V^{(S)} = 0.3G_S$ is $(331.3, 19)$MeV. There is no TCP at $G_V^{(S)} = 0.6G_S$. The characteristics of this graph is similar to that of Figure 6.5. Once again, the phase boundary favors the second order phase transition as $G_V^{(S)}$ increases. In this case, the second order phase transition at $G_V^{(S)} = 0.6G_S$ is so dominant that there is no TCP in the phase boundary. Therefore, there is no first order transition in the entire phase boundary at $G_V^{(S)} = 0.6G_S$.

Figures 6.4-6.6 show that the behavior of the phase boundary and TCP at increasing $G_V^{(S)}$ is the same at zero magnetic field and at constant magnetic field. Although this behavior

is only studied using parameter values from Table 1 Set A, it is expected that a similar behavior would occur for Table 2 Set A. The main difference is the actual numerical values of the TCP would be different.

It is significant to address the kinks that exist in several of the curves after the location of the TCP and/or in the region of high chemical potentials. The phase boundary is located by finding the onset of chiral symmetry restoration when approaching from the broken phase; thus the solution at $M = 0$ at the second order phase transition is utilized. Since a second order phase transition solution is used to approximate the entire phase boundary, the points that belong in the first order phase transition are not as certain as the points in the second order phase transition. It is not reliable whether the part of the phase boundary after the TCP is weakly first order for all the curves at different parameters (eB, G_S, $G_V^{(S)}$). However, the location of the TCP is certain since it is a matter of determining the point at which the second order phase transition ends.

7 Conclusions

In this thesis, the effects a magnetic field has on the phase boundary, where the spontaneously broken chiral symmetry is restored, are studied using a two-flavor NJL model. Additionally, the modified model is also used to explore the effects a magnetic field has on the location of the TCP, where the order of the chiral phase transition changes from second order to first order. The phase boundaries and the TCP for u and d quarks are calculated at various magnetic fields in order to investigate the relationship between phase transition and magnetic field. Moreover, the phase boundaries and the TCP for u and d quarks are compared at the same magnetic field in order to study the effect the quark electric charge has on the phase transition. It is also significant to change the coupling constant $G_V^{(S)}$ and observe how it affects the phase transition.

When a magnetic field is present, the phase boundary of the u quark and the phase boundary of the d quark are no longer the same curve in comparison to the case of zero magnetic field. Instead, there are two phase boundaries, one for each quark, due to the difference in electric charge in Eq. (5.4). Both phase boundaries shift to higher chemical potentials and temperatures compared to the phase boundary at zero magnetic field, with the u quark having a slightly higher phase boundary curve than the d quark.

As the magnetic field increases, the phase boundaries for both u and d quarks shift to higher temperatures and chemical potentials. The change in the location of the TCP demonstrates that the phase boundary favors the first order phase transition as the magnetic field increases. On the other hand, at constant magnetic field and increasing $G_V^{(S)}$ the phase boundaries of the u and d quarks favor the second order phase transition. Thus, increasing $G_V^{(S)}$ causes a favoring of the second order phase transition.

In the future, it would be interesting to explore the behavior of the dynamical mass M_u and M_d in relation to magnetic fields and temperatures (fixed chemical potential) or to magnetic fields and chemical potentials (fixed temperature). Hence, in this case, the solution at $M = 0$

at the second order phase transition would not be the only solution studied. In addition, the expression for the energy of u and d quarks in Eq. (5.4) would also depend on M_u and M_d. Furthermore, the magnetic fields discussed in this thesis are only in the region of strong magnetic fields. Small magnetic fields should also be studied in order to confirm the behaviors of the phase boundary and the location of the TCP at zero magnetic field.

References

[1] K. Fukushima and T. Hatsuda, Rept. Prog. Phys. 74 (2011) 014001.

[2] K. Rajagopal and F. Wilczek. The condensed matter physics of QCD. arXiv:hep-ph/0011333, 2000.

[3] F.R. Brown, et al., Phys. Rev. Lett. 65 (1990) 2491.

[4] M. Asawaka and Y. Yazaki, Nucl. Phys. A 504 (1989) 668.

[5] A. Barducci, et al., Phys. Rev. D 49 (1994) 426.

[6] M.A. Halasz, et al., Phys. Rev. D 58 (1998) 096007.

[7] J. Bergues and K. Rajagopal, Nucl. Phys. B 538 (1999) 215.

[8] O. Scavenius, A. Mocsy, I.N. Mishustin and D.H. Rischke, Phys. Rev. C 64 (2001) 045202.

[9] B.J. Schaefer and J. Wabach, Phys. Rev. D 75 (2007) 085015.

[10] P. Costa, M.C. Ruivo and C.A. Sousa, Phys. Rev. D 77 (2008) 096001.

[11] Y. Hatta and T. Ikeda, Phys. Rev. D 67 (2003) 014028

[12] C. Sasaki, B. Friman and K. Redlich, Phys. Rev. D 75 (2007) 054026.

[13] D.J. Griffiths. Introduction to elementary particles. New York: Wiley, 1987.

[14] T. Schafer. Phases of QCD. arXiv:hep-ph/0509068, 2005.

[15] L.D. Landau and E.M. Lifshitz, Statistical Physics, Course of Theoretical Physics Vol. 5. New York: Pergamon Press, 1980.

[16] D. Scheffler. NJL model study of the QCD phase diagram using the Taylor series expansion technique. Darmstadt: Institut für Kernphysik, 2007.

[17] M. Buballa, Phys. Rep. 407 (2005) 0402234.

[18] P. Kernan, G.D. Starkman, and T. Vachaspati. Phys. Rev. D 54 (1996) 9509126.

Appendix

//program to find phase boundary at M=0 for different sets of parameters; no magnetic field

```
#include <stdio.h>
#include <stdlib.h>
#include <string.h>
#include <math.h>
#define PI 3.14159265
#define max_in 1001 // max number of intervals
#define vmin 0.0 // ranges of integration
//#define vmax 664.3
//#define vmax 797.2
#define vmax 995.5
double f(double p, double chemP, double Temp);
double trapez (int no, double min, double max, double chemP, double Temp);
int main()
{
double result, beta;
int i, j, k, l;
double integrand, integration_value, comparison;
double percentage_difference= 0.0005;
int numColors=3;
FILE *output;
output= fopen("phase_boundary_setC.txt", "w");
//coupling constants and cutoff
// double p_cutoff= 664.3; //MeV
// double p_cutoff= 797.2; //MeV
double p_cutoff= 995.5; //MeV
// double cutoff= 4.124; // G_S*lambda^2
// double cutoff= 3.871; // G_S*lambda^2
double cutoff= 3.659; // G_S*lambda^2
double G_S= cutoff/pow(p_cutoff,2);
//quark chemical potential
```

```
double shifted_max_qChem_potential= 325.0; //MeV
double shifted_qChem_potential_step_size= 1.0; //MeV
int shifted_qChem_potential_matrix= (shifted_max_qChem_potential/

shifted_qChem_potential_step_size);

double shifted_qChem_potential[shifted_qChem_potential_matrix];
//Temperature
double max_T= 180.0;
double T_step_size= 1.0;
int T_matrix= (max_T/T_step_size);
double T[T_matrix];
for(i=0; i<= shifted_qChem_potential_matrix; i++)
{
shifted_qChem_potential[i+1]= shifted_qChem_potential[i]+shifted_qChem_potential_step_size;
}
for(j=0; j<= T_matrix; j++)
{
T[j+1]= T[j]+T_step_size;
}
integration_value= (pow(PI,2)/(2.0*G_S*numColors));
printf("%lf\n", integration_value);
// cycle through fixed values of mu and T to find solutions
for (k=0; k<= T_matrix; k++)
{
for (j=0; j<=shifted_qChem_potential_matrix; j++)
{
for (i = 3; i< max_in; i+= 2)
{
result= trapez(i, vmin, vmax, shifted_qChem_potential[j], T[k]);
}
if( fabs(result-integration_value)/integration_value <= percentage_difference)
{
fprintf(output, "%lf\t%lf\n", shifted_qChem_potential[j], T[k]);
}
```

```
}
}
fclose(output);
return 0;
}
// function to integrate
double f(double p, double chemP, double Temp)
{
double integrand;
double beta= 1/Temp;
integrand= p*( 1.0- 1/(1+exp(beta*(p-chemP))) - 1/(1+exp(beta*(p+chemP))) ); // at phase boundary, M=0
return (integrand);
}
double trapez (int no, double min, double max, double chemP, double Temp)
{
// trapezoid rule
int n;
double interval, sum = 0.0, p;
interval= ((max-min) / (no-1));
for (n = 2; n<no; n++)
{ // sum the midpoints
p = interval * (n-1);
sum += f(p, chemP, Temp)*interval;
}
sum += 0.5 *(f(min, chemP, Temp) + f(max, chemP, Temp)) * interval; // add the endpoints
return (sum);
}
```

```
//program to find tricritical point of phase boundary; no magnetic field; find a=b=0
#include <stdio.h>
#include <stdlib.h>
#include <string.h>
#include <math.h>
#define PI 3.14159265
#define max_in 1001 // max number of intervals
#define vmin 0.0 // ranges of integration
#define vmin_b 0.1
//#define vmax 664.3
//#define vmax 797.2
#define vmax 995.5
double f_a(double p, double chemP, double Temp);
double f_b(double p, double chemP, double Temp);
double trapez_a(int no, double min, double max, double chemP, double Temp);
double trapez_b(int no, double min, double max, double chemP, double Temp);
int main()
{
double result_a, result_b;
int i, j, k, l;
double a, b;
int numColors=3;
FILE *output, *input;
// output= fopen("TCP_setA_0.txt", "w");
// output= fopen("TCP_setB_0.txt", "w");
output= fopen("TCP_setC_0.txt", "w");

// input= fopen("phase_boundary_setA.txt", "r");
// input= fopen("phase_boundary_setB.txt", "r");
input= fopen("phase_boundary_setC.txt", "r");
//coupling constants and cutoff
// double p_cutoff= 664.3; //MeV
// double p_cutoff= 797.2; //MeV
double p_cutoff= 995.5; //MeV
```

```
// double cutoff= 4.124; // G_S*lambda^2
// double cutoff= 3.871; // G_S*lambda^2
double cutoff= 3.659; // G_S*lambda^2
double G_S= cutoff/pow(p_cutoff,2);
// double G_V= 0.3*G_S;
double shifted_chem, T, M, chem_potential;
double constant_value_a= (1.0*numColors)/pow(PI,2);
double constant_value_b= (3.0*numColors)/pow(PI,2);
while (fscanf(input, "%lf\t%lf\n", &shifted_chem, &T) != EOF)
{
for (i = 3; i< max_in; i+= 2)
{
result_a= trapez_a(i, vmin, vmax, shifted_chem, T);
result_b= trapez_b(i, vmin_b, vmax, shifted_chem, T);
}
a= (1/(2.0*G_S))- (constant_value_a*result_a);
b= constant_value_b*result_b;
fprintf(output, "%lf\t%lf\t%lf\t%lf\n", shifted_chem, T, a, b);
}
fclose(output);
fclose(input);
return 0;
}
// second derivative=a; find value of a
double trapez_a(int no, double min, double max, double chemP, double Temp)
{
// trapezoid rule for a
int n;
double interval, sum_a = 0.0, p;
interval= ((max-min) / (no-1));
for (n = 2; n<no; n++)
{ // sum the midpoints
p = interval * (n-1);
```

```
sum_a += f_a(p, chemP, Temp)*interval;
}
sum_a += 0.5 *(f_a(min, chemP, Temp) + f_a(max, chemP, Temp)) * interval; // add the endpoints
return (sum_a);
}
//function to integrate for a
double f_a(double p, double chemP, double Temp)
{
double integrand_a;
double beta= 1/Temp;
integrand_a= p* (1- 1/(1+exp(beta*(p-chemP))) - 1/(1+exp(beta*(p+chemP))) ) ;
return (integrand_a);
}

//4th derivative=b; find value of b

double trapez_b (int no, double min, double max, double chemP, double Temp)
{
// trapezoid rule
int n;
double interval, sum_b= 0.0, p;
interval= ((max-min) / (no-1));
for (n = 2; n<no; n++)
{ // sum the midpoints
p = interval * (n-1);
sum_b += f_b(p, chemP, Temp)*interval;
}
sum_b += 0.5 *(f_b(min, chemP, Temp) + f_b(max, chemP, Temp)) * interval; // add the endpoints
return (sum_b);
}
// function to integrate for b
double f_b(double p, double chemP, double Temp)
{
```

```
double integrand_b;
double beta= 1/Temp;
integrand_b= (1/p)* (1- 1/(1+exp(beta*(p-chemP))) - 1/(1+exp(beta*(p+chemP))) ) ;
return (integrand_b);
}
```

//program to find the phase boundary for the down quark in the chiral limit at various magnetic fields; M=0 solution in the second order phase transition; similar program for up quark

```
#include <stdio.h>
#include <stdlib.h>
#include <string.h>
#include <math.h>
#define PI 3.14159265
#define max_in 100000 // max number of intervals
#define vmin 0.0
#define vmin_0 0.1 // ranges of integration
#define vmax 664.3
//#define vmax 797.2
//#define vmax 995.5
double Simpsons_Rule_Sum_LR_q( double a, double h, int n, int l, double eB, double q, double chem, double T );
double f_q(double p, int l, double eB, double q, double chem, double T);
int main()
{
int i, j, k, l;
double integrand, integration_value, comparison, constant_value;
double percentage_difference= 0.0005;
double vacuum, max;
int numColors=3;
FILE *output;
output= fopen("phase_boundary_setA_200_down.txt", "w");
//coupling constants and cutoff
double p_cutoff= 664.3; //MeV
// double p_cutoff= 797.2; //MeV
// double p_cutoff= 995.5; //MeV
double cutoff= 4.124; // G_S*lambda^2
// double cutoff= 3.871; // G_S*lambda^2
// double cutoff= 3.659; // G_S*lambda^2
double G_S= cutoff/pow(p_cutoff,2);
```

```
double eB= pow(200.0,2); // user input what eB is;
double q= 1.0/3.0;
int limiting_int= (int)(pow(p_cutoff,2)/(2.0*q*eB)); //highest Landau level in summation of l
printf("%i\n", limiting_int);
double height;
double height0= (vmax-vmin_0)/max_in;

//quark chemical potential
double shifted_max_qChem_potential= 305.0; //MeV
double shifted_qChem_potential_step_size= 0.5; //MeV
int shifted_qChem_potential_matrix= (shifted_max_qChem_potential/

shifted_qChem_potential_step_size);

double shifted_qChem_potential[shifted_qChem_potential_matrix];

//Temperature
double max_T= 180.0;
double T_step_size= 0.5;
int T_matrix= (max_T/T_step_size);
double T[T_matrix];
for(i=0; i<= shifted_qChem_potential_matrix; i++)
{
shifted_qChem_potential[i+1]= shifted_qChem_potential[i]+shifted_qChem_potential_step_size;
}
for(j=0; j<= T_matrix; j++)
{
T[j+1]= T[j]+T_step_size;
}
integration_value= (1.0*PI*PI)/(2.0*G_S*numColors*q*eB);
double sum0=0.0, sum=0.0, result_q=0.0, result=0.0;
printf("integration values down= %lf\n", integration_value);
// cycle through fixed values of mu and T to find solutions
for (k=0; k<= T_matrix; k++)
{
for (j=0; j<=shifted_qChem_potential_matrix; j++)
```

```
{
sum0= 0.0;
sum=0.0;
result= result_q= 0.0;
sum0= 0.5*Simpsons_Rule_Sum_LR_q(vmin_0, height0, max_in, 0, eB, q,

shifted_qChem_potential[j], T[k]);

for(l=1; l<=limiting_int; l++)
{
max= sqrt(p_cutoff*p_cutoff-2.0*q*eB*l);
if(max>=0)
{
height= (max-vmin)/max_in;
sum= Simpsons_Rule_Sum_LR_q(vmin, height, max_in, l, eB, q, shifted_qChem_potential[j],
T[k]);
result_q= result_q+sum;
}
}
result_q= result_q+sum0;
//compare values to integration value
if( fabs((result_q-integration_value)/integration_value) <= percentage_difference)
{
fprintf(output, "%lf\t%lf\n", shifted_qChem_potential[j], T[k]);
}

}

}

fclose(output);
return 0;
}
//Simpsons Rule summed from left to right to evaluate integrals
double Simpsons_Rule_Sum_LR_q( double a, double h, int n, int l, double eB, double q, double
chem, double T )
{
```

```
double h2 = 0.5 * h;
double bound = a + (n - 0.25) * h;
double integral = f_q(a, l, eB, q, chem, T) + 4.0 * f_q(a + h2, l, eB, q, chem, T );

for (a += h; a < bound; a += h)
integral += 2.0 * f_q(a, l, eB, q, chem, T) + 4.0 * f_q(a + h2, l, eB, q, chem, T);
return 0.16666666666666666667 * h * ( integral + f_q(a, l, eB, q, chem, T) );
}

// function to integrate
double f_q(double p, int l, double eB, double q, double chem, double T)
{
double integrand;
double beta= 1.0/T;
integrand=((1.0)/sqrt(p*p+2.0*q*eB*l))*(1.0-1.0/(1+exp(beta*(sqrt(p*p+2.0*q*eB*l)- chem)))-

1.0/(1+exp(beta*(sqrt(p*p+2.0*q*eB*l)+chem))) );

return (integrand);
}
```

//program to find TCP of up phase boundary at different magnetic fields; similar program for down quark

```
#include <stdio.h>
#include <stdlib.h>
#include <string.h>
#include <math.h>
#define PI 3.14159265
#define max_in 100000 // max number of intervals
#define vmin 0.0 // ranges of integration
#define vmax 664.3
//#define vmax 797.2
//#define vmax 995.5
#define vmin_0 0.1
double Simpsons_Rule_Sum_LR_q( double a, double h, int n, int l, double eB, double q, double chem, double T );
double f_q(double p, int l, double eB, double q, double chem, double T);
int main()
{
int i, j, k, l;
double integrand, integration_value, comparison, constant_value;
double vacuum, max;
int numColors=3;
FILE *output, *input;
input= fopen("phase_boundary_setA_200_up.txt", "r");
output= fopen("TCP_setA_200_up.txt", "w");
//coupling constants and cutoff
double p_cutoff= 664.3; //MeV
// double p_cutoff= 797.2; //MeV
// double p_cutoff= 995.5; //MeV
double cutoff= 4.124; // G_S*lambda^2
// double cutoff= 3.871; // G_S*lambda^2
// double cutoff= 3.659; // G_S*lambda^2
double G_S= cutoff/pow(p_cutoff,2);
double eB= pow(200.0,2); // user input what eB is;
```

```
double q= 2.0/3.0;
int limiting_int= (int)(pow(p_cutoff,2)/(2.0*q*eB));
printf("%i\n", limiting_int);
double height;
// double height=(vmax-vmin)/max_in;
double height0= (vmax-vmin_0)/max_in;
double T, chem_potential, shifted_chem;
constant_value= (3.0*numColors*q*eB)/(PI*PI); //constant with coupling constant
printf("constant value= %lf\n", constant_value);
double sum0=0.0, sum=0.0, result_q=0.0, result=0.0;
while (fscanf(input, "%lf\t%lf\n", &shifted_chem, &T) != EOF)
{
sum0= 0.0;
sum=0.0;
result= result_q= 0.0;
sum0= 0.5*Simpsons_Rule_Sum_LR_q(vmin_0, height0, max_in, 0, eB, q, shifted_chem, T);
for(l=1; l<=limiting_int; l++)
{
max= sqrt(p_cutoff*p_cutoff-2.0*q*eB*l);
if(max>=0)
{
height= (max-vmin_0)/max_in;
sum= Simpsons_Rule_Sum_LR_q(vmin, height, max_in, l, eB, q, shifted_chem, T);
result_q= result_q+sum;
}
}
result_q= result_q+sum0;
result= constant_value*result_q;
fprintf(output, "%lf\t%lf\t%lf\n", shifted_chem, T, result);
}
fclose(output);
return 0;
}
//find value of b
```

```
double Simpsons_Rule_Sum_LR_q( double a, double h, int n, int l, double eB, double q, double
chem, double T )
{
double h2 = 0.5 * h;
double bound = a + (n - 0.25) * h;
double integral = f_q(a, l, eB, q, chem, T) + 4.0 * f_q(a + h2, l, eB, q, chem, T );
for (a += h; a < bound; a += h)
integral += 2.0 * f_q(a, l, eB, q, chem, T) + 4.0 * f_q(a + h2, l, eB, q, chem, T);
return 0.16666666666666666667 * h * ( integral + f_q(a, l, eB, q, chem, T) );
}
// 4th derivative
double f_q(double p, int l, double eB, double q, double chem, double T)
{
double integrand;
double beta= 1.0/T;
integrand=(1.0/pow(p*p+2.0*q*eB*l,1.5))*(1.0-(exp(chem/T)*(exp(sqrt(p*p+2.0*q+eB*l))*

(sqrt(p*p+2.0*q+eB*l)+T)+T*exp(chem/T))/((exp(beta*(sqrt(p*p+2.0*q*eB*l)))+exp(chem/T))*

(exp(beta*(sqrt(p*p+2.0*q*eB*l)))+exp(chem/T))))-((sqrt(p*p+2.0*q+eB*l)+T)*

(exp(beta*(sqrt(p*p+2.0*q*eB*l)+chem))+T)/((1+exp(beta*(sqrt(p*p+2.0*q*eB*l)+chem)))*

(1+exp(beta*(sqrt(p*p+2.0*q*eB*l)+chem))))) );

return (integrand);
}
```

//program to find TCP of up phase boundary at different magnetic fields; similar program for down quark

```
#include <stdio.h>
#include <stdlib.h>
#include <string.h>
#include <math.h>
#define PI 3.14159265
#define max_in 100000 // max number of intervals
#define vmin 0.0 // ranges of integration
#define vmax 664.3
//#define vmax 797.2
//#define vmax 995.5
#define vmin_0 0.1
double Simpsons_Rule_Sum_LR_q( double a, double h, int n, int l, double eB, double q, double chem, double T );
double f_q(double p, int l, double eB, double q, double chem, double T);
int main()
{
int i, j, k, l;
double integrand, integration_value, comparison, constant_value;
double vacuum, max;
int numColors=3;
FILE *output, *input;
input= fopen("phase_boundary_setA_200_up.txt", "r");
output= fopen("TCP_setA_200_up.txt", "w");
//coupling constants and cutoff
double p_cutoff= 664.3; //MeV
// double p_cutoff= 797.2; //MeV
// double p_cutoff= 995.5; //MeV
double cutoff= 4.124; // G_S*lambda^2
// double cutoff= 3.871; // G_S*lambda^2
// double cutoff= 3.659; // G_S*lambda^2
double G_S= cutoff/pow(p_cutoff,2);
double eB= pow(200.0,2); // user input what eB is;
```

```
double q= 2.0/3.0;
int limiting_int= (int)(pow(p_cutoff,2)/(2.0*q*eB));
printf("%i\n", limiting_int);
double height;
// double height=(vmax-vmin)/max_in;
double height0= (vmax-vmin_0)/max_in;
double T, chem_potential, shifted_chem;
constant_value= (3.0*numColors*q*eB)/(PI*PI); //constant with coupling constant
printf("constant value= %lf\n", constant_value);
double sum0=0.0, sum=0.0, result_q=0.0, result=0.0;
while (fscanf(input, "%lf\t%lf\n", &shifted_chem, &T) != EOF)
{
sum0= 0.0;
sum=0.0;
result= result_q= 0.0;
sum0= 0.5*Simpsons_Rule_Sum_LR_q(vmin_0, height0, max_in, 0, eB, q, shifted_chem, T);
for(l=1; l<=limiting_int; l++)
{
max= sqrt(p_cutoff*p_cutoff-2.0*q*eB*l);
if(max>=0)
{
height= (max-vmin_0)/max_in;
sum= Simpsons_Rule_Sum_LR_q(vmin, height, max_in, l, eB, q, shifted_chem, T);
result_q= result_q+sum;
}
}
result_q= result_q+sum0;
result= constant_value*result_q;
fprintf(output, "%lf\t%lf\t%lf\n", shifted_chem, T, result);
}
fclose(output);
return 0;
}
//find value of b
```

```
double Simpsons_Rule_Sum_LR_q( double a, double h, int n, int l, double eB, double q, double
chem, double T )
{
double h2 = 0.5 * h;
double bound = a + (n - 0.25) * h;
double integral = f_q(a, l, eB, q, chem, T) + 4.0 * f_q(a + h2, l, eB, q, chem, T );
for (a += h; a < bound; a += h)
integral += 2.0 * f_q(a, l, eB, q, chem, T) + 4.0 * f_q(a + h2, l, eB, q, chem, T);
return 0.16666666666666666667 * h * ( integral + f_q(a, l, eB, q, chem, T) );
}
// 4th derivative
double f_q(double p, int l, double eB, double q, double chem, double T)
{
double integrand;
double beta= 1.0/T;
integrand=(1.0/pow(p*p+2.0*q*eB*l,1.5))*(1.0-(exp(chem/T)*(exp(sqrt(p*p+2.0*q+eB*l))*

(sqrt(p*p+2.0*q+eB*l)+T)+T*exp(chem/T))/((exp(beta*(sqrt(p*p+2.0*q*eB*l)))+exp(chem/T))*

(exp(beta*(sqrt(p*p+2.0*q*eB*l)))+exp(chem/T))))-

((sqrt(p*p+2.0*q+eB*l)+T)* (exp(beta*(sqrt(p*p+2.0*q*eB*l)+chem))+T)/

((1+exp(beta*(sqrt(p*p+2.0*q*eB*l)+chem)))* (1+exp(beta*(sqrt(p*p+2.0*q*eB*l)+chem))))) );

return (integrand);
}
```

//program to find phase boundary at different G_V coupling constant; no magnetic field

```
#include <stdio.h>
#include <stdlib.h>
#include <string.h>
#include <math.h>
#define PI 3.14159265
#define max_in 1001 // max number of intervals
#define vmin 0.0 // ranges of integration
#define vmax 995.5
double f(double p, double chemP, double Temp);
double trapez (int no, double min, double max, double chemP, double Temp);
int main()
{
double result;
int i, j, k, l;
double integrand, constant_value, comparison;
int numColors=3;
FILE *output, *input;
output= fopen("Eqn_214_M0_setC_0.6.txt", "w");
input= fopen("Eqn_213_M0_setC.txt", "r");
//coupling constants and cutoff
double p_cutoff= 995.5; //MeV
double cutoff= 1.829; // G_S*lambda^2
double G_S= cutoff/pow(p_cutoff,2);
double G_V= 0.6*G_S;
double shifted_chem, T, M, chem_potential;
constant_value= (4.0*G_V*numColors)/pow(PI,2); //left hand side of comparison
while (fscanf(input, "%lf\t%lf\n", &shifted_chem, &T) != EOF)
{
for (i = 3; i< max_in; i+= 2)
{
result= trapez(i, vmin, vmax, shifted_chem, T);
}
```

```
result= constant_value*result;
chem_potential= shifted_chem+ result;
fprintf(output, "%lf\t%lf\t%lf\n", shifted_chem, chem_potential, T);
}
fclose(output);
fclose(input);
return 0;
}
// function to integrate
double f(double p, double chemP, double Temp)
{
double integrand;
double beta= 1/Temp;
integrand= p*p*(1/(1+exp(beta*(p-chemP))) - 1/(1+exp(beta*(p+chemP))) );
return (integrand);
}
double trapez (int no, double min, double max, double chemP, double Temp)
{
// trapezoid rule
int n;
double interval, sum = 0.0, p;
interval= ((max-min) / (no-1));
for (n = 2; n<no; n++)
{ // sum the midpoints
p = interval * (n-1);
sum += f(p, chemP, Temp)*interval;
}
sum += 0.5 *(f(min, chemP, Temp) + f(max, chemP, Temp)) * interval; // add the endpoints
return (sum);
}
```

//program to find phase boundary at different G_V coupling constant; with magnetic field; up quark

```
#include <stdio.h>
#include <stdlib.h>
#include <string.h>
#include <math.h>
#define PI 3.14159265
#define max_in 100000 // max number of intervals
#define vmin 0.0 // ranges of integration
#define vmax 664.3
#define vmin_0 0.0

double Simpsons_Rule_Sum_LR_q( double a, double h, int n, int l, double eB, double q, double chem, double T );
double f_q(double p, int l, double eB, double q, double chem, double T);
int main()
{
int i, j, k, l;
double integrand, constant_value, comparison;
int numColors=3;
FILE *output, *input;
output= fopen("Eqn_214_250_up_0.6.txt", "w");
input= fopen("phase_boundary_setA_250_up.txt", "r");
//coupling constants and cutoff
double p_cutoff= 664.3; //MeV
double cutoff= 2.060; // G_S*lambda^2
double G_S= cutoff/pow(p_cutoff,2);
double G_V= 0.6*G_S;
double eB= pow(250.0,2); // user input what eB is;
double q= 2.0/3.0;
int limiting_int= (int)(pow(p_cutoff,2)/(2.0*q*eB));
double shifted_chem, T, chem_potential;
constant_value= (2.0*G_V*numColors*q*eB)/pow(PI,2); //left hand side of comparison
```

```
printf("constant value= %lf\n", constant_value);
double height, sum0, sum, result, result_q, max;
double height0= (vmax-vmin_0)/max_in;
while (fscanf(input, "%lf\t%lf\n", &shifted_chem, &T) != EOF)
{
sum0= 0.0;
sum=0.0;
result= result_q= 0.0;
sum0= 0.5*Simpsons_Rule_Sum_LR_q(vmin_0, height0, max_in, 0, eB, q, shifted_chem,
T);
for(l=1; l<=limiting_int; l++)
{
max= sqrt(p_cutoff*p_cutoff-2.0*q*eB*l);
if(max>=0)
{
height= (max-vmin)/max_in;
sum= Simpsons_Rule_Sum_LR_q(vmin, height, max_in, l, eB, q, shifted_chem, T);
result_q= result_q+sum;
}
}
result= sum0+result_q;
chem_potential= shifted_chem+ constant_value*result;
fprintf(output, "%lf\t%lf\t%lf\n", shifted_chem, chem_potential, T);
}
fclose(output);
fclose(input);
return 0;
}
double Simpsons_Rule_Sum_LR_q( double a, double h, int n, int l, double eB, double q,
double chem, double T )
{
double h2 = 0.5 * h;
```

```
double bound = a + (n - 0.25) * h;
double integral = f_q(a, l, eB, q, chem, T) + 4.0 * f_q(a + h2, l, eB, q, chem, T );
for (a += h; a < bound; a += h)
integral += 2.0 * f_q(a, l, eB, q, chem, T) + 4.0 * f_q(a + h2, l, eB, q, chem, T);
return 0.16666666666666666667 * h * ( integral + f_q(a, l, eB, q, chem, T) );
}

// function to integrate
double f_q(double p, int l, double eB, double q, double chem, double T)
{
double integrand;
double beta= 1.0/T;
integrand= ( 1.0/(1+exp(beta*(sqrt(p*p+2.0*q*eB*l)-chem))) -

1.0/(1+exp(beta*(sqrt(p*p+2.0*q*eB*l)+chem))) );

return (integrand);
}
```

Curriculum Vitae

Lidens Cheng was born in Phnom Penh, Cambodia on October 24, 1989. The only child of Sophea Mak and Chakyra Cheng, she moved to the United States in 1998 at the age of 9. She graduated from Orange High School, Orange, California in the summer of 2007. In the spring of 2011, she graduated Cum Laude from Illinois Institute of Technology with a Bachelor of Science degree in physics and minor in applied mathematics. In the fall of 2011, she joined the University of Texas at El Paso to pursue a Master of Science degree in physics. During her study at UTEP, she conducted research in high energy physics and nuclear theory.